

Ge redistribution in SiO₂/SiGe structures under thermal oxidation: Dynamics and predictions

Ethan Long, , Alexander Azarov, , Frode Kløw, , Augustinas Galeckas, , Andrej Yu Kuznetsov, and , and Spyridon Diplas

Citation: *Journal of Applied Physics* **111**, 024308 (2012); doi: 10.1063/1.3677987

View online: <http://dx.doi.org/10.1063/1.3677987>

View Table of Contents: <http://aip.scitation.org/toc/jap/111/2>

Published by the [American Institute of Physics](#)

Articles you may be interested in

[A kinetic model for the oxidation of silicon germanium alloys](#)

Journal of Applied Physics **98**, 074904 (2005); 10.1063/1.2060927

AIP | Journal of
Applied Physics

Save your money for your research.
It's now **FREE** to publish with us -
no page, color or publication charges apply.

Publish your research in the
Journal of Applied Physics
to claim your place in applied
physics history.

Ge redistribution in SiO₂/SiGe structures under thermal oxidation: Dynamics and predictions

Ethan Long,^{1,a)} Alexander Azarov,¹ Frode Kløw,¹ Augustinas Galeckas,¹ Andrej Yu Kuznetsov,¹ and Spyridon Diplas²

¹*Department of Physics/Center for Materials Science and Nanotechnology, University of Oslo, P.O. Box 1048 Blindern, Oslo N-0316, Norway*

²*SINTEF Materials and Chemistry, Oslo N-0314, Norway and Department of Chemistry/Center for Materials Science and Nanotechnology, University of Oslo, P.O. Box 1048 Blindern, Oslo N-0316, Norway*

(Received 29 August 2011; accepted 15 December 2011; published online 24 January 2012)

Several fundamental aspects of the oxidation-induced redistribution of Ge in thin films of SiGe are studied. This includes the incorporation of Ge into the oxide and the formation of what is alternatively referred to as pile-up, snow-plow, or a germanium-rich layer. Experimental data from the present work shows longer oxidation times leading to an increase of Ge content in the pile-up region and eventually creating a single high Ge content pile-up layer by entirely consuming the initial SiGe layer. The pile-up effect was shown to occur at the oxidation interface, with the highest Ge content occurring at the same interface. For a given oxide thickness, the redistribution of Ge and the formation of a pile-up region was shown experimentally to be independent of temperature in the range between 800 °C and 1000 °C. Simulations using common models for the oxidation of Si and diffusion of Si in SiGe indicate that temperature does have an influence on the composition of the pile-up layer, though the range of achievable compositions is limited. The flux of Si due to diffusion of Si in SiGe relative to the oxidation-induced flux of Si out of the SiGe is integral to the formation and dimensions of a pile-up region. Two predictive relations were derived for describing the dynamics of oxidation of SiGe. The first relation is given for determining the pile-up layer thickness as a function of oxide thickness and the composition of the pile-up layer. The second relation assumes a limited supply of Si and is for determination of the minimum initial thickness of a SiGe layer to avoid oxidation of Ge. The validity of these equations was confirmed experimentally by RBS and XPS data from the present work. The proposed models may be used in nanostructuring of thin films of SiGe by oxidation and in the design of core-shell structures and transistors. This is all done with a focus on oxidation of epitaxial thin films (< 100 nm) of Si_{1-x}Ge_x in dry O₂ at 1 atm between 800 °C and 1000 °C. © 2012 American Institute of Physics. [doi:10.1063/1.3677987]

I. INTRODUCTION

The importance of SiGe in IC design and fabrication is increasing due to demand for higher speed and lower power electronics, recent commercialization of FINFETs, advances in the fabrication of SiGe-on-insulator¹⁻³ (sapphire or SiO₂), and the proliferation of RF applications in the marketplace. Incorporation of Ge into Si CMOS processing has been motivated by SiGe's utility in creating high mobility channels,⁴ reduction of parasitic effects, like drain-induced barrier lowering,⁵ and creation of other novel gate architectures and nanowire transistors.^{6,7} Yet another promising application of SiGe is its use in core-shell structures for photovoltaics.⁸ Nanostructuring of SiGe by oxidation is an effective method for construction of a wide variety of SiGe-based electronic devices, a fact which highlights the importance of research into the dynamics of oxidation of SiGe and the subsequent redistribution of Ge in the SiGe.

The use of dry O₂ oxidation to create SiGe core-shell structures relies on the selective oxidation of Si, which acts

to separate Si from Ge and creates a graded Ge concentration in the SiGe. Such concentration gradients are typically characterized by a Ge-rich region adjacent to the SiO₂ growth front and are variously referred to as a pile-up region, snow plow effect, or germanium-rich layer (GRL). The pile-up effect, resulting from dry oxidation of SiGe, has been reported to occur in numerous publications,⁹⁻²³ but these observations are frequently limited to the acknowledgment of the existence of a pile-up layer. Furthermore, the reports do not provide sufficient information to understand how modification of the oxidation conditions may lead to variations in the profile of Ge concentration in the SiGe.

The present work addresses the dynamics of oxidation of thin films of SiGe by considering dry O₂ oxidation with various times and temperatures. The focus on sub-100-nm films ensures that the discussion is pertinent to modern technological applications.

The driving factors in the formation of a pile-up layer are, first, the susceptibility for incorporation of Ge into the oxide and, second, the relative diffusion of O, Si, and Ge in the oxidizing material. The Ge content of the oxide is evaluated here using analysis of x ray photoelectron spectroscopy (XPS) data.

^{a)}Author to whom correspondence should be addressed. Electronic mail: ethanl@smn.uio.no.

The role of Gibbs energies in the formation of oxides is reviewed to provide a better understanding of the influence of temperature on the incorporation of Ge into the oxide. The relative diffusion of oxidant in SiO₂ and that of Si in SiGe or Ge forms the basis of several models that have been proposed to describe the oxidation processes in SiGe.^{23–26} The present work uses Rutherford backscattering spectroscopy (RBS) data to evaluate the role of oxidation time and temperature in the formation of a pile-up region and to provide experimental support for two descriptive relations. The proposed relations describe the pile-up layer thickness as a function of oxide thickness and allow prediction of the initial SiGe layer thickness required to avoid oxidation of Ge. These models may be useful in making first order estimates in the design of core-shell structures and transistors using oxidized SiGe.

II. EXPERIMENTAL

Epitaxial layers of Si_{1-x}Ge_x on a 100-nm Si buffer layer were grown on (100)-oriented Si substrates. The Si_{1-x}Ge_x layer thicknesses for the two wafers used were 80 nm and 70 nm for $X=0.15$ and $X=0.20$, respectively. The thermal oxidation was done using a tube furnace at ambient pressure flushed with dry O₂ at 800 °C, 850 °C, 900 °C, 950 °C, and 1000 °C. The native oxides were not removed prior to oxidation.

X ray photoelectron spectroscopy (XPS) was performed with a *Kratos Axis Ultra DLD* system using Al K α x ray excitation ($h\nu=1486.6$ eV). Compositional profiles were acquired by combining XPS measurements with Ar⁺ cation etching. The XPS compositional profiles were correlated to physical depths using profilometer measurements of the milled craters. The resolution of XPS measurements is given by the detection depth, $d=3\lambda\cos\theta$, where λ is the inelastic mean free path of photoelectrons and θ is the angle of emission. In this case, θ is 0°, so the detection depth is 3.5 nm for the Ge2p photoelectrons, which is significantly less than the detection depth of 11.7 nm for Ge3d photoelectrons. These detection depth values were derived assuming that the photoelectrons are traveling through an SiO₂ layer and by using data from the Tanuma, Powell, and Penn algorithm.^{27,28}

Rutherford backscattering spectroscopy (RBS) measurements were done with 2 MeV 4He⁺ ions backscattered into the detector at 100° relative to the incident beam direction.

This glancing-angle detector geometry was used to provide enhanced depth resolution for accurate analysis of films near the surface region. Oxide and pile-up layer thicknesses were determined by fitting simulated curves to the experimentally determined RBS spectra.

Oxide thicknesses were also measured by ellipsometry at 632.8 nm and 830.0 nm wavelengths and 70° angle of incidence, with each sample repeatedly measured at each wavelength in order to account for random error in the measurements. The analysis used a three-layer model and treated the oxide, pile-up, and SiGe layer thicknesses as well as the index of refraction for the pile-up layer as unknowns. For the purpose of comparing the oxide thicknesses determined by ellipsometry to those determined by RBS, the certainty in the ellipsometry measurements may be calculated while presuming the RBS values to be the actual values. With such a presumption, the sample standard deviation in the ellipsometry measurements was calculated to be 3.8 nm.

III. RESULTS AND DISCUSSION

A. Oxide composition

A critical factor in the manipulation of Ge concentrations in SiGe thin films by oxidation is the degree to which Ge is incorporated into the oxide. Considering this, Fig. 1 shows an XPS depth profile of the oxide of a Si_{0.85}Ge_{0.15} sample oxidized at 950 °C for 25 min. Ar⁺ cation etching was used to expose progressively deeper levels of the sample to create the depth profile of the sample composition shown. A short etch time was used for this sample to highlight the composition of the oxide. In the XPS profiles, metallic and oxidized Si appear at binding energies of ~97 eV and ~102 eV, while metallic and oxidized Ge appear at ~1215 eV and ~1219 eV, respectively. Noting that Ge2p photoelectrons have low kinetic energy and arise from shallow depths, the surface sensitive Ge2p peak indicates that the native oxide contains some oxidized Ge, which is consistent with other reports in the literature.²⁹ The remainder of the oxide is devoid of any form of Ge until the SiO₂ to SiGe interface is reached.

XPS data in Fig. 2 illustrates very similar behavior for a sample with a comparable oxide thickness, but oxidized at 850 °C. A long etch time was used for this sample, so the XPS profile shows the sample composition from the surface

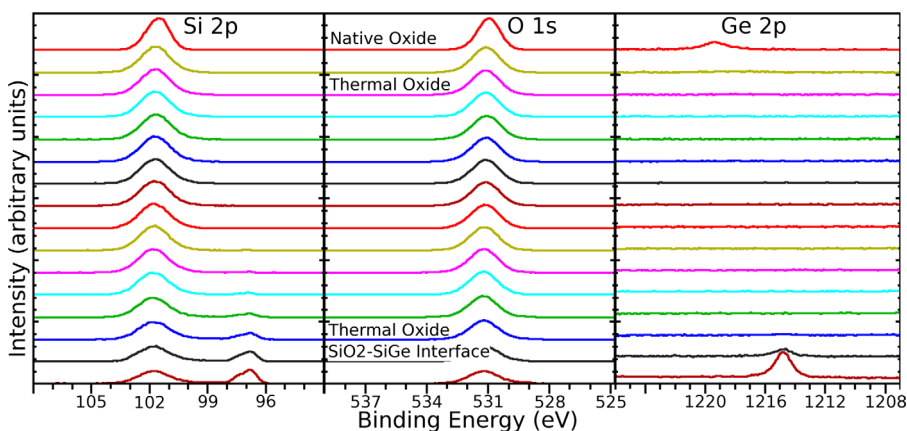


FIG. 1. (Color online) XPS depth profile of a Si_{0.85}Ge_{0.15} thin film oxidized at 950 °C for 25 min. The oxide thickness as measured by ellipsometry is 392 Å. The topmost profile is for the surface of the unetched sample. The bottom-most profile is at the SiGe layer, as indicated by the presence of metallic Si and Ge.

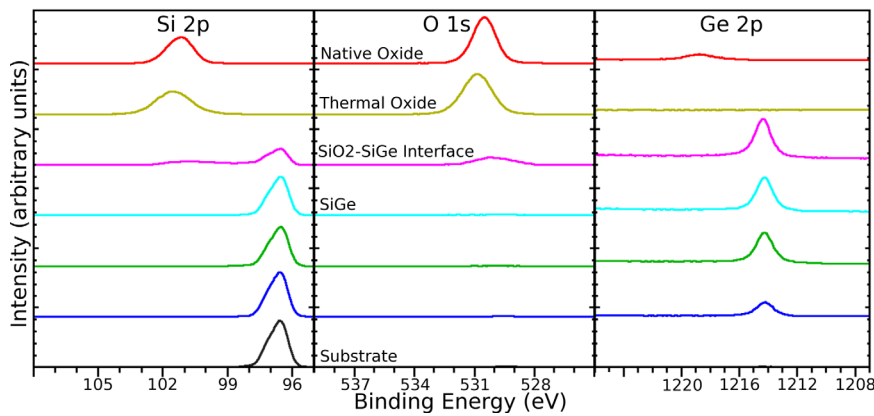


FIG. 2. (Color online) XPS depth profile of $\text{Si}_{0.85}\text{Ge}_{0.15}$ thin film oxidized at 850°C for 75 min. The oxide thickness as measured by ellipsometry is 356 \AA . The topmost profile is for the unetched sample surface. The bottommost profile is at the substrate, as indicated by the presence of metallic Si and the absence of either O or Ge.

all the way to the substrate. It can be seen that GeO_2 appears in the region of the native oxide, while only SiO_2 occurs in the bulk of the oxide. Metallic Ge can be seen in the SiGe layer, and no Ge is present in the substrate. However, when compared to the sample in Fig. 1, the longer etching times used between XPS measurements for the sample in Fig. 2 result in less detailed probing of the interface between the oxide and pile-up layers.

Figure 3 presents a depth profile showing the relative concentrations of O, Si, and Ge constructed from the same XPS data as was used for Fig. 2; the lines connecting data points in Fig. 3 are for illustrative purposes only. The depth profile uses the Ge3d signal, which is less surface sensitive than the Ge2p signal, but allows better comparison to the O and Si data due to the fact that the signals arise from similar depths.

Figure 3 does indicate the presence of Ge in the region of the native oxide, but considering the limited resolution of the Ge3d peak, the concentration of Ge in this region is negligibly small. Both Figs. 1 and 2 also indicate that the GeO_2 is limited to the native oxide. This is consistent with experimental evidence presented in the literature showing GeO_2 in very thin or low temperature oxides, including native oxides.^{30–32} Also, there is a point of high Ge concentration at the interface between the oxide and SiGe layers, which is indicative of a Ge pile-up layer with a Ge concentration that is roughly double that of the intrinsic SiGe.

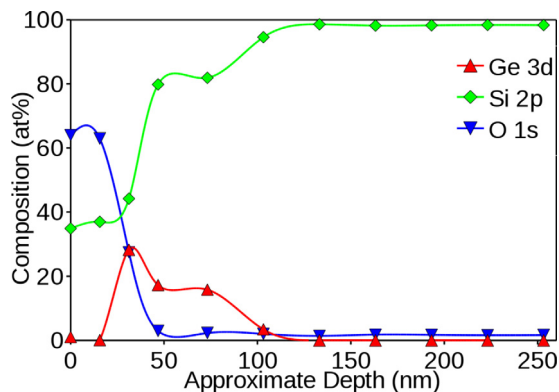


FIG. 3. (Color online) Profile of $\text{Si}_{0.85}\text{Ge}_{0.15}$ oxidized at 850°C for 75 min showing relative atomic composition vs depth from XPS measurements. The oxide thickness as measured by ellipsometry is 356 \AA .

The preferential oxidation of Si over that of Ge is a critical characteristic of SiGe oxidation and can be explained using the Gibbs energies, G , of the constituent reactants.³² Thus, an understanding of the Gibbs energies involved will help explain whether Ge will be incorporated into the oxide during thermal oxidation.

The change in Gibbs energy due to a reaction between several reactants is given by $\Delta G_P = G_P - (G_{R1} + G_{R2})$, where G_P , G_{R1} , and G_{R2} are the Gibbs energies of the reaction product and two separate reactants, respectively.³³ A negative value for ΔG_P indicates that the reaction will occur spontaneously. The values of ΔG_{SiO_2} and ΔG_{GeO_2} for the formation of oxide from Si, Ge, and O_2 for temperatures between 27°C and 1127°C are in the range of -856 kJ/mol to -661 kJ/mol and -521 kJ/mol to -310 kJ/mol ,³³ respectively. It is clear that, although both SiO_2 and GeO_2 formation are exergonic, the SiO_2 reaction is more so than that of GeO_2 , leading to the preferential formation of SiO_2 . This point may be emphasized by the data in Fig. 4, showing ΔG_{SiO_2} for the formation of SiO_2 from GeO_2 and Si, which is equivalent to the difference between ΔG_{SiO_2} and ΔG_{GeO_2} . The data in Fig. 4 shows that SiO_2 is preferred over GeO_2 , at least for temperatures between 27°C and 1127°C , and that any occurrence of GeO_2 may be converted to SiO_2 , given elemental Si.³⁴ This preference is exaggerated at higher temperatures, but ΔG is consistently and substantially negative between temperatures where native oxides might occur and the upper end of common oxidation temperatures. This and other published analyses³² indicate that Ge will not be oxidized if elemental Si is present.

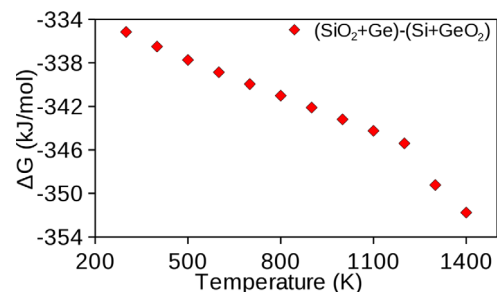


FIG. 4. (Color online) Gibbs energies for the formation of SiO_2 from GeO_2 and Si (Ref. 33).

The analysis of the thermodynamics of Si and Ge oxidation is useful in determining whether Ge will be oxidized in such a tertiary system, but it does not address the question of whether there is a tertiary system, that is, whether Si is present at the oxidation interface. The supply of Si to the oxidizing interface, and thus the exclusive oxidation of Si versus oxidation of both Si and Ge, depends on the diffusion of the constituent species in the thin films. This has been examined by modeling the flows of oxidant through the oxide and of Si through a Ge-rich region adjacent to the oxidizing interface.^{22,23,32} Low relative Si flows induced by low temperatures or high oxidant pressures have been recognized as leading to formation of GeO₂.^{30,32} Kilpatrick *et al.*²³ have determined a so-called crossover temperature for various oxide thicknesses and oxidation conditions, below which GeO₂ is formed and above which the oxide is exclusively SiO₂. For dry oxidation at 1 atm, this crossover temperature is listed as ~380 °C for very thin oxides and not exceeding ~650 °C for oxides of a few micrometers or more.²³

The presence of oxidized Ge in the native oxide, as demonstrated in Figs. 1 and 2, may be due to the low diffusion rates of Si and Ge as compared to O at such low temperatures. If Si is fixed due to low diffusion rates at low temperatures during the formation of the native oxide, the surface of the SiGe film would be denuded of metallic Si, allowing for the oxidation of Ge. The very fast oxidation rates for ultrathin oxides during subsequent thermal oxidation may prevent diffusion of enough Si to the outermost surface of the oxide to convert the oxidized Ge to SiO₂ according to the thermodynamics presented in Fig. 4. The Si2p line at the sample surface in both Figs. 1 and 2 confirm the absence of metallic Si in this layer. This may be contrasted to the interface region between the thermal oxide and the SiGe layer. In this interface region, the Si2p and O1s lines indicate the coexistence of Si and SiO₂, while the Ge2p line indicates the absence of any oxidized Ge, which lends further credence to the conclusions presented in Fig. 4 and the accompanying discussion.

The oxidation temperatures used in this study and those that appear most commonly in the literature are between 800 °C and 1000 °C. This is motivated in part by the fact that lower temperatures increase the probability of Ge incorporation into the oxide, which will reduce the pile-up effect and potentially compromise the electrical integrity of the oxide. On the other hand, higher temperatures could lead to melting of the pile-up region, which may have an adverse effect on the oxidation process;^{21–23} the melting temperature for Ge is ~940 °C, with the solidus curve passing Si_{0.25}Ge_{0.75} at ~1000 °C.³⁵

B. Ge redistribution and the pile-up layer

Given that Ge incorporation into the oxide is not significant under the oxidation conditions considered here, our focus on evaluation of the Ge concentration profile shifts to the SiGe layer, from which Si is leached during oxidation. Figure 3 has shown that a region of elevated Ge concentration occurs at the oxidation front. This pile-up effect has been reported at temperatures as low as 600 °C²³ and as high as 1125 °C.¹³ Li *et al.*²⁰

examined the Ge concentration at the oxidation interface for different oxidation temperatures and times and qualitatively compared the influence of temperature on the oxidation rate to the diffusion of Ge. However, the authors did not examine the Ge concentration away from the interface to give a better description of the overall Ge distribution. A few reports present profiles of Ge distributions for various oxidation times at individual temperatures;^{18–21} an approach which is useful for understanding the progression of the pile-up effect over time. Figure 5 takes this approach by presenting data from the present study, showing RBS profiles from Si_{0.80}Ge_{0.20} samples oxidized for various times at 900 °C with an emphasis on the Ge signal. The RBS profiles represent samples with oxide thicknesses between the native oxide for the un-oxidized sample and 575 Å for a sample oxidized for 150 min at 900 °C. The inset shows a wide view of two RBS spectra, including the O, Si, and Ge signals for the un-oxidized and most oxidized samples. In the case of oxidation for 25 min resulting in a 196 Å oxide, there is a distinct pile-up region that is clearly differentiated from the bulk of the SiGe layer. At 67 min (356 Å oxide), the pile-up continues to enhance the Ge concentration and, although there is a Ge gradient, there are not two distinct regions of Ge concentration. At 150 min (575 Å oxide), there is only a single region of high Ge concentration. In the latter sample, there is clearly a pile-up effect, but the resulting stoichiometry is fundamentally different from the dual concentration regions frequently associated with the terms pile-up, snow plow, and germanium-rich layer (GRL) and that are required by core-shell structures.

Figure 6 shows the RBS profiles for Si_{0.85}Ge_{0.15}, wherein the channel number has been normalized in such a way as to align the oxide to SiGe interface for all of the samples. This is done in order to illustrate more clearly the development of the pile-up region. The tendency for longer oxidation times to induce higher Ge concentrations is clearly visible. Furthermore, whereas in the non-oxidized sample, the Ge concentration near the oxidation front gradually increases to a plateau value, the longer the sample is oxidized, the steeper the RBS profile becomes at the oxide to SiGe interface. This indicates that the RBS resolution is not

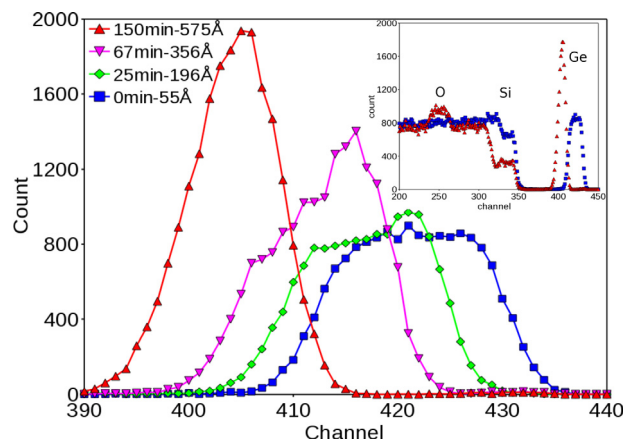


FIG. 5. (Color online) RBS profiles of Ge concentration for Si_{0.80}Ge_{0.20} oxidized at 900 °C for various times, including an un-oxidized sample. The inset shows two spectra with a broader range, including signals for O, Si, and Ge for two samples with very thin and thick oxides. The spectra are labeled by oxidation time and oxide thickness (from ellipsometry).

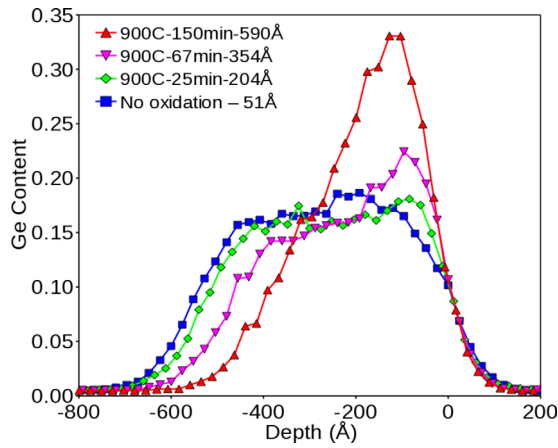


FIG. 6. (Color online) Ge content vs depth from RBS measurements for $\text{Si}_{0.85}\text{Ge}_{0.15}$ samples with various oxide thicknesses. Excepting the unoxidized sample, the oxidation temperature was 900°C . The profiles are aligned with the oxidation front at depth zero. The spectra are labeled by oxidation temperature, time, and oxide thickness (from ellipsometry.)

the sole cause for the gradual increase in Ge for the intrinsic samples and that oxidation serves to maximize the Ge concentration at the oxidation front. In contrast, the slope of the RBS profile for the Ge at the interface with the substrate remains reasonably constant with oxidation time. This along with the fact that the depth of the Ge profile decreases with time indicates that there is little or no diffusion of Ge into the substrate. It is possible that oxidation of thicker intrinsic SiGe layers would demonstrate this more clearly by ensuring a longer plateau and distance between the pile-up region and the substrate.

Another approach is presented by Jang *et al.*,¹⁴ who look at pile-up effects at multiple temperatures for a single oxidation time. Although most authors conclude that temperature does influence the Ge profile, they do not effectively compare one temperature to another, because the use of one oxidation time for multiple temperatures results in different amounts of Si having been removed from the SiGe layer by oxidation. To fully appreciate the influence of temperature on the Ge distribution, samples with similar oxide thicknesses should be compared such that the Si removed from the SiGe layer by oxidation is similar for all samples and temperatures. Figure 7 shows such data from $\text{Si}_{0.85}\text{Ge}_{0.15}$ samples with similar oxide thicknesses which were oxidized at temperatures between 800°C and 1000°C . There is no clearly discernible influence of temperature on the Ge concentration profile for a given oxide thickness.

C. Empirical relations for layer thicknesses

The thicknesses of the pile-up and oxide layers that result from thermal oxidation may be determined using ellipsometry, RBS, or TEM. However, it is useful for the experimentalist or technologist to have a simple predictive tool for determining these values before an oxidation is done. To that end, the following discussion presents two relations that may be used in designing nanostructures in oxidized thin films of SiGe.

The term “pile-up” is in fact poorly defined in the literature and can only be described reliably as the tendency to increase the Ge concentration in a region adjacent to the oxidation front. This does not define the Ge profile other than to state that it is higher than it was prior to oxidation. The magnitude and profile of the germanium concentration in the pile-up region will depend on a balance between the oxidation rate and the rate of diffusion of Si through the pile-up region toward the oxidation front. If, however, this system is simplified by removing the effect of the diffusion of Si and also assuming that the pile-up region is 100% Ge, then the thickness of the pile-up region can be calculated directly.

Considering the oxidation of Si; the depth of Si consumed, $t_{\text{Si-consumed}}$, in order to provide enough Si for the formation of an oxide with thickness t_{ox} , is described as

$$t_{\text{Si-consumed}} = t_{\text{ox}}N_{\text{ox}}/N_{\text{Si}}, \quad (1)$$

where N_{ox} and N_{Si} are the molecular and atomic densities of the oxide and Si, respectively. Similarly, for the oxidation of SiGe, the depth of SiGe from which Si is extracted to form the oxide layer, $t_{\text{SiGe-consumed}}$, is

$$t_{\text{SiGe-consumed}} = t_{\text{ox}}N_{\text{ox}}/N_{\text{Si-SiGe}}, \quad (2)$$

where $N_{\text{Si-SiGe}}$ is the atomic density of Si in the SiGe layer; this assumes exclusive oxidation of Si. If the composition of the initial SiGe layer is described by X , the number of Ge atoms in the SiGe as a fraction of the total, while the total atomic density of the SiGe is N_{SiGe} , then the atomic densities of Si and Ge in the SiGe are

$$N_{\text{Si-SiGe}} = N_{\text{SiGe}}(1 - X) \text{ and } N_{\text{Ge-SiGe}} = N_{\text{SiGe}}X \quad (3)$$

or

$$N_{\text{Ge-SiGe}} = N_{\text{Si-SiGe}}X(1 - X)^{-1}. \quad (4)$$

If all of the Si atoms are removed from the SiGe layer to a depth of $t_{\text{SiGe-consumed}}$, leaving a layer of pure Ge (i.e., no Si), then

$$N_{\text{Ge-SiGe}}t_{\text{SiGe-consumed}} = N_{\text{Ge}}t_{\text{pileup}}, \quad (5)$$

where N_{Ge} is the atomic density of Ge and t_{pileup} is the thickness of the pile-up region. The pile-up thickness may then be found by substitution as

$$t_{\text{pileup}} = Xt_{\text{ox}}N_{\text{ox}}[(1 - X)N_{\text{Ge}}]^{-1}. \quad (6)$$

Here, the pile-up layer is composed only of Ge, and so t_{pileup} is at its minimum possible value. As the pile-up layer will inevitably contain some Si, Eq. (6) may be rewritten as

$$\begin{aligned} t_{\text{pileup}} &= Xt_{\text{ox}}N_{\text{ox}}[(1 - X)N_{\text{Ge-pileup}}]^{-1} \\ &= Xt_{\text{ox}}N_{\text{ox}}[(1 - X)X_{\text{pileup}}N_{\text{SiGe-pileup}}]^{-1}, \end{aligned} \quad (7)$$

where $N_{\text{Ge-pileup}}$ is the atomic density of Ge in the pile-up layer, $N_{\text{SiGe-pileup}}$ is the atomic density of the pile-up layer, and X_{pileup} is the fraction of Ge in the pile-up layer. Equation (7) is a more

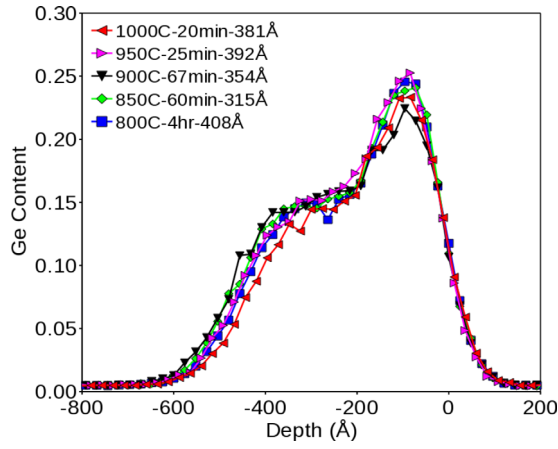


FIG. 7. (Color online) Ge content vs depth from RBS measurements for oxidized $\text{Si}_{0.85}\text{Ge}_{0.15}$ samples with similar oxide thicknesses but varying oxidation temperatures. The profiles are aligned with the oxidation front at depth zero and labeled according to oxidation temperature, time, and oxide thickness (from ellipsometry.)

general expression and is equivalent to Eq. (6) when $X_{\text{pileup}} = 1$.

Equation (6), wherein the pile-up layer is composed entirely of Ge, may serve as a limiting condition, particularly when considering oxidation of SiGe-on-insulator or when oxidizing nanorods. These are situations in which there will be no diffusion of Si from the substrate and, thus, a limited supply of Si for oxidation. Oxidation of such structures beyond a given oxide thickness will lead to the oxidation of Ge due to the absence of Si for oxidation. Three cases can be defined for SiGe-on-insulator systems (with the pre-oxidation SiGe layer thickness written as $t_{\text{SiGe-initial}}$):

- i. $t_{\text{ox}} > [t_{\text{SiGe-initial}}(1-X)N_{\text{SiGe}}/N_{\text{ox}}]$; formation of GeO_2 ;
- ii. $t_{\text{ox}} = [t_{\text{SiGe-initial}}(1-X)N_{\text{SiGe}}/N_{\text{ox}}]$; maximum pile-up before GeO_2 formation;
- iii. $t_{\text{ox}} < [t_{\text{SiGe-initial}}(1-X)N_{\text{SiGe}}/N_{\text{ox}}]$; Ge pile-up and only SiO_2 .

The minimum initial SiGe thickness required to avoid formation of GeO_2 in SiGe-on-insulator systems is then

$$t_{\text{SiGe-initial}} = t_{\text{SiGe-consumed}} = t_{\text{ox}}N_{\text{ox}}[(1-X)N_{\text{SiGe}}]^{-1}, \quad (8)$$

where N_{SiGe} may be determined through a quadratic fit to the data presented in Dismukes *et al.*,³⁶ $N_{\text{SiGe}} = (5.0214 - 0.5286X - 0.0517X^2)10^{22}$ atoms/cm³. The assumptions made in arriving at Eq. (8) mandate that absolutely all of the Si in the SiGe layer is oxidized prior to oxidation of Ge. However, Kilpatrick *et al.*²³ point out that Ge and Si will oxidize simultaneously when the flow of O to the oxidation interface outweighs the flow of Si to the same interface. So, in practice, the minimum initial SiGe layer thickness to avoid formation of GeO_2 will be somewhat larger than is predicted by Eq. (8), but it will not be any smaller. For the fabrication of nanowires, consideration of the dimensions of the nanowire must take into account the fact that oxidation will occur from multiple dimensions as well as the likelihood that oxidation will occur at different rates for

different crystal facets. This is a similar problem for FINFETS, but, in this case, an oxidation barrier like a SiN cap may be placed on top of the fin in order to limit oxidation to two sides.

The discussion so far has not incorporated diffusion of Si from the substrate. In the event that Si does diffuse toward the oxide from the substrate, some of the Si from the SiGe layer that has been incorporated into the oxide during oxidation will effectively be replaced by Si diffusing from the substrate into the SiGe layer. This effect can be expressed by rearranging Eq. (7) to show the dose of Si in the oxide and that removed from the SiGe layer with the addition of the dose of Si from the substrate, Q_{sub} ,

$$Q_{\text{sub}} + t_{\text{pileup}}N_{\text{SiGe-pileup}}X_{\text{pileup}}(1-X)/X = t_{\text{ox}}N_{\text{ox}}. \quad (9)$$

The present work and other studies^{15–17,37} have used samples with SiGe on Si and provide enough data to give a cursory validation of Eq. (9). Figure 8 uses data from this study as well as data extracted from published work to plot the dose of Si in the oxide, $t_{\text{ox}}N_{\text{ox}}$, versus the dose of Si removed from the SiGe, $t_{\text{pileup}}N_{\text{SiGe-pileup}}X_{\text{pileup}}(1-X)/X$. The value used for N_{ox} in Fig. 8 is 2.21×10^{22} Si atoms/cm³, and the data therein is separated and labeled by the Ge content of the pre-oxidation SiGe layer and the data source.

In the event that Q_{sub} is 0, the dose in the oxide should exactly equal the dose from the pile-up region, and the correlation between the two should have a slope of 1. The data in Fig. 8 shows that this is the case for the small oxide thicknesses, but that the data for larger oxide thicknesses indicate a non-zero value for Q_{sub} . This is quite sensible for the case of small oxide thicknesses, as very little if any of the Si from the substrate will have reached the pile-up or oxide due to the relatively thick SiGe layer it must pass through and the short oxidation time associated with the thin oxide. Regarding the thicker oxides; if all other values are correct, then the value of Q_{sub} indicated would have to be negative, which is not easily explicable, given that Si from the substrate should diffuse into and not out of the SiGe. However, the accuracy with which the variables in Eq. (9) are determined is not perfect, and the results are particularly susceptible to variation in the value used for X . Furthermore, what constitutes the

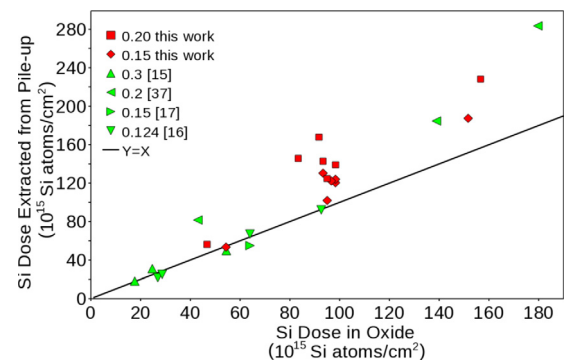


FIG. 8. (Color online) Si dose extracted from the pile-up region, $t_{\text{pileup}}N_{\text{SiGe-pileup}}X_{\text{pileup}}(1-X)/X$, vs that in the oxide, $t_{\text{ox}}N_{\text{ox}}$, from Eq. (9) with data from this study and other works (Refs. 15–17 and 37). All data points are labeled by the initial Ge content. The oxide and pile-up thickness data from this study are extracted from RBS measurements. The black diagonal in the plot indicates where the x-values equal the y-values.

thickness of the pile-up region is not well defined in the literature. Smaller values of the pile-up thickness, concentration, or density would help to account for the apparent negative value of Q_{sub} in Fig. 8. The same is true of larger values of the oxide thickness or density or of the initial SiGe concentration. It is clear though that there is no evidence of diffusion of Si from the substrate making any substantial contribution to the dimensions of the oxide or pile-up layer.

D. Determination of the pile-up Ge concentration

The system being discussed can be described by three fundamental fluxes of Si. The first is the flux of Si being consumed by the oxide, J_{ox} , the second is the flux of Si from the SiGe region through the pile-up toward the oxidation front, J_{pileup} , while the third is the flux of Si from the substrate into the SiGe region, $J_{substrate}$.

The relationship between J_{ox} and J_{pileup} is integral to the formation of the pile-up region. Where $J_{ox} > J_{pileup}$, a pile-up region will form, and if this condition remains true for long enough, both Si and Ge will be oxidized and X_{pileup} will be 1, whereas $J_{ox} < J_{pileup}$ will lower the Ge concentration at the oxidation front. The case in which $J_{ox} = J_{pileup}$ will affect a constant Ge concentration at the oxidation front.

The diffusivity of Si in Ge is reported as being five to six orders of magnitude higher than the diffusivity of Si in Si.³⁸ This will tend to create an abrupt transition between the SiGe region and the pile-up region with nearly constant Ge concentration in the pile-up region. If at first a pile-up region composed entirely of Ge is formed and J_{ox} is both independent of X_{pileup} and less than J_{pileup} , the Ge concentration in the pile-up region will decrease, thereby decreasing J_{pileup} until either $J_{pileup} = J_{ox}$ or until the pile-up concentration equals the concentration of the infinite source (the initial SiGe concentration in this case.) In this way, X_{pileup} is determined by balancing the flux of silicon to the oxidation front and the flux of silicon consumed by oxidation and can be considered a single value because of the assumption of an abrupt transition between the SiGe layer and the pile-up layer. This makes the oxidation rate a determining factor in the formation of the pile-up region.

The relationship between $J_{substrate}$ and J_{pileup} are synonymous to that between J_{pileup} and J_{ox} . Given that the diffusivity of Si in Ge is orders of magnitude higher than it is in Si and that a pile-up region exists with a Ge concentration that is higher than the initial SiGe concentration, the condition where $J_{substrate} > J_{pileup}$ should never occur. It would then also be true that lower initial Ge concentrations will minimize the contribution of $J_{substrate}$ to the formation of the pile-up region. More precisely, the contribution of $J_{substrate}$ to the formation of the pile-up will decrease as the ratio X/X_{pileup} goes from 1 to 0. In the extreme case where $X = 1$ and $J_{substrate} = 0$, there is no Si to be oxidized and no pile-up region. This situation may be extended to any condition in which $X/X_{pileup} > 1$, whether $X = 1$ or $X_{pileup} < X < 1$. The implication of this is that, if J_{ox} acts to limit the value of X_{pileup} to less than 1, then there will exist a maximum value of X , below which a pile-up region may form and above which no pile-up will occur. The case where X is very close to 0

will minimize the influence of $J_{substrate}$ and will maximize the pile-up effect by maximizing the contrast between the Ge concentration in the initial SiGe layer and the pile-up region (i.e., minimizing the X/X_{pileup} ratio). Thicker initial layers of SiGe will also minimize the influence of $J_{substrate}$.

If the Ge concentration is constant throughout the pile-up region and the entirety of the Si in the pile-up region and the oxide is considered to be supplied by diffusion of Si, then the post oxidation Ge content may be written as the sum of doses from diffusion and the doses in the resulting oxide and pile-up region,

$$\begin{aligned} Q_{diffusion} &= Q_{ox} - Q_{sub} + Q_{pileup} \\ &= (Q_{ox} - Q_{sub})\{1 + (1 - X_{pileup})X/[X_{pileup}(1 - X)]\}, \end{aligned} \quad (10)$$

where $Q_{diffusion}$ is the dose of Si supplied to the pile-up from J_{pileup} (i.e., from the initial SiGe layer), $Q_{ox} = t_{ox}N_{ox}$ is the dose of Si in the oxide, and $Q_{pileup} = t_{pileup}N_{SiGe-pileup}(1 - X_{pileup})$ is the dose of Si remaining in the pile-up region after oxidation. Substitution of t_{pileup} from Eq. (9) allows the simplification of Eq. (10).

Figure 9 shows the values of X_{pileup} that satisfy Eq. (10) versus the oxide thickness; the data presented is for five temperatures and is labeled accordingly. The value of t_{ox} , and thus Q_{ox} , for various oxidation times and temperatures is found by modeling the oxide thickness with the Massoud³⁹ model while using oxidation rate constants for Si published therein. The value of $Q_{diffusion}$ is determined using a pre-deposition diffusion model while defining the initial SiGe layer as the infinite source and the pile-up layer as the medium into which Si is diffusing. The diffusivity of Si in the said medium is defined by X_{pileup} and is estimated from published values.³⁸ The initial SiGe region is thick (e.g., ~ 100 nm) and has a low value of X (0.05), such that the contribution of $J_{substrate}$ to the formation of the oxide and pile-up layer may be neglected. Use of a Ge concentration, X , of 5% for the initial SiGe layer also ensures that the assumptions of an infinite source associated with a pre-deposition model and Si oxidation constants are appropriate approximations. The flatness of the curves in Fig. 9 reflect a close correlation between J_{ox} and J_{pileup} , except for oxide thicknesses very close to 0.

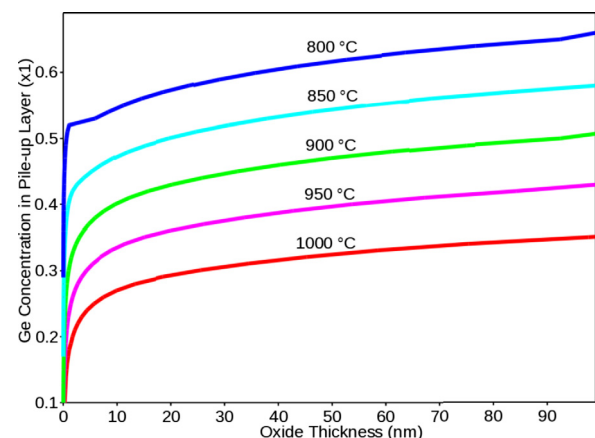


FIG. 9. (Color online) Ge concentration in the pile-up layer, X_{pileup} , that satisfies Eq. (10) vs the oxide thickness.

The influence of X_{pileup} on the relationship between J_{ox} and J_{pileup} may be seen by considering the ratio between the left- and right-hand sides of Eq. (10). Figure 10 shows this ratio as a function of oxide thickness (analogous to oxidation time), as determined by the Massoud³⁹ model. The data presented is for five values of X_{pileup} and is labeled accordingly, while X is fixed at 0.05 and the temperature is fixed at 1000 °C. A value of 1 indicates the Ge concentration for which Eq. (10) is satisfied. Small changes in X_{pileup} cause a drastic deviation from the equilibrium condition, where the scaled ratio of doses is 1. The value of X_{pileup} that satisfies Eq. (10) remains quite stable over a range of oxide thicknesses.

Figure 11 shows the same scaled ratio of doses for the same five values of X_{pileup} as in Fig. 10, but plotted against temperature and for a fixed oxide thickness of 50 nm. Figure 11 suggests that X_{pileup} has a limited dependence on temperature, though the data in Fig. 7 suggest that this dependence is substantially smaller. The stability of the value of X_{pileup} over a range of oxidation thicknesses suggested by Figs. 9 and 10 and the results in Fig. 11 suggest that there is a limited range of pile-up concentrations that may be achieved by oxidation in the sub-100-nm region and particularly in the linear oxidation regime, which is dominated by a nearly constant oxidation rate.

This analysis suggests that variation of the oxidation temperature during the oxidation could be a realistic means to control the pile-up concentration, but that the range of achievable pile-up concentrations is limited. In discussion of their own modeling results, Kilpatrick *et al.*²³ also mention the limited dependence of X_{pileup} on temperature, but they do not demonstrate the point. If temperature variation is used to control the pile-up concentration, the pile-up thickness could be controlled by modification of the oxidation time and the initial SiGe concentration. However, wet oxidation or controlled oxidant pressure would be more effective methods of controlling X_{pileup} , as they act to modify the oxidation rate without simultaneously altering the diffusion of Si in SiGe, as happens with temperature changes.

E. Oxidation rate dependence on pile-up concentration

The discussion, so far, has assumed that the oxidation rate of SiGe alloys is the same as or close to that of Ge-free

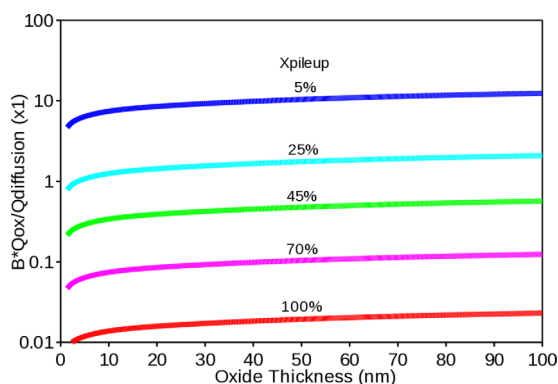


FIG. 10. (Color online) A plot of the scaled ratio of doses from Eq. (10) vs oxide thickness. Here, $B = \{1 + (1 - X_{pileup})X/[X_{pileup}(1 - X)]\}$.

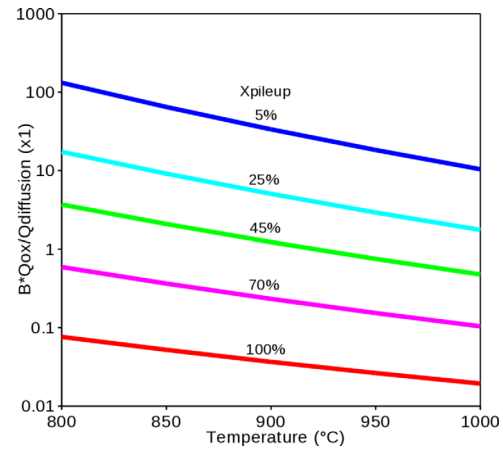


FIG. 11. (Color online) A plot of the scaled ratio of doses from Eq. (10) vs temperature. Here, $B = \{1 + (1 - X_{pileup})X/[X_{pileup}(1 - X)]\}$.

Si and may be described by the Massoud³⁹ or Deal and Grove⁴⁰ models. If the oxidation rate of SiGe is enhanced or slowed as a function of Ge concentration, then the pile-up layer concentration will be integral to determining the oxidation rate. Recognizing that higher Ge concentrations act as a catalyst for diffusion of Si in SiGe alloys, if variation in Ge concentrations influence the oxidation rate of SiGe, then the two effects will create a feedback loop between J_{ox} and J_{pileup} . With the starting assumption that $J_{ox} = J_{pileup}$ and since higher Ge concentrations lead to higher fluxes of Si in SiGe, there are five cases to consider for comparison of the rate of change of flux with respect to Ge concentration in the pile-up:

- i. $dJ_{pileup}/dX_{pileup} < dJ_{ox}/dX_{pileup}$; the thermodynamic preference for oxidation of Si will initiate an increase in X_{pileup} , leading to $J_{ox} > J_{pileup}$ and then to $X_{pileup} = 1$ and the oxidation of Ge
- ii. $dJ_{pileup}/dX_{pileup} = dJ_{ox}/dX_{pileup}$; published values³⁸ for diffusivity of Si in SiGe and a common model, like the pre-deposition model, would lead to orders of magnitude difference in the oxidation rate of SiGe between $X = 0$ and $X = 1$. The data from this study does not support this case.
- iii. $dJ_{pileup}/dX_{pileup} > dJ_{ox}/dX_{pileup} > 0$; an increase in X_{pileup} causes a smaller value of J_{ox}/J_{pileup} , which leads to a disproportionately large drop in X_{pileup}
- iv. $dJ_{pileup}/dX_{pileup} > dJ_{ox}/dX_{pileup} = 0$; although an increase in X_{pileup} will increase J_{pileup} , no feedback occurs and J_{ox} is unaffected
- v. $-dJ_{pileup}/dX_{pileup} < dJ_{ox}/dX_{pileup} < 0$; an increase in X_{pileup} causes a larger value of J_{ox}/J_{pileup} , which leads to a disproportionately large increase in X_{pileup}
- vi. $-dJ_{pileup}/dX_{pileup} > dJ_{ox}/dX_{pileup}$; an initial increase in X_{pileup} leads to a lower oxidation rate, J_{ox}/J_{pileup} , and X_{pileup} . The associated drop in J_{pileup} is not sufficient to compensate for the drop in J_{ox} , and X_{pileup} is forced toward X , making the pile-up layer disappear.

If Ge acts as either a catalyst or inhibitor for the oxidation of Si in SiGe alloys, then the oxidation rate will vary as a function of X_{pileup} . Holland *et al.*²⁶ recognize this point and

suggest that a difference in binding energy of Si to Si and Si to Ge at the oxidation front is responsible for Ge acting as a catalyst. However, their analysis relies on correlation of Ge implant doses (i.e., X) to oxide thickness rather than explicitly correlating oxidation rate to X_{pileup} . The influence of X , temperature, time, pressure, and the oxidation ambient on oxidation rate must be decoupled from their influence on X_{pileup} in order to determine how and whether Ge acts as a catalyst or inhibitor for oxidation of Si.

IV. SUMMARY AND CONCLUSIONS

This study addresses several fundamental aspects of the oxidation-induced redistribution of Ge in thin films of SiGe, including the incorporation of Ge into the oxide and the formation of what is alternatively referred to as pile-up, snow-pow, or a germanium-rich layer. The dynamics of the formation of a pile-up layer are explored, with attention given to the influence of oxidation temperature on Ge redistribution and formation of a pile-up region. This is done with novel observations and is motivated by the use of thermal oxidation for nanostructuring and device fabrication with SiGe. The analysis is supported by experimental evidence from RBS, XPS, and ellipsometry measurements, as well as simulations. The focus of the study is on oxidation of epitaxial thin films (< 100 nm) of $Si_{1-x}Ge_x$ in dry O_2 at 1 atm and $800^\circ C$, $850^\circ C$, $900^\circ C$, $950^\circ C$, and $1000^\circ C$.

The oxidization of SiGe in the temperature range between $800^\circ C$ and $1000^\circ C$ at ambient pressures has been demonstrated to avoid the incorporation of Ge into the SiO_2 layer. As predicted by an analysis of the Gibbs free energies, the preferential oxidation of Si is supported by observations made by XPS. The XPS profiles show limited oxidized Ge in the native oxide, while no oxidized Ge is present in the thermal oxide or the Si-rich region of the SiGe to SiO_2 interface.

RBS data shows longer oxidation times, leading to an increase of Ge content in the pile-up region and eventually creating a single high Ge content pile-up layer by entirely consuming the initial SiGe layer. The pile-up effect was shown to occur at the oxidation interface, with the highest Ge content occurring at the same interface. For a given oxide thickness, the redistribution of Ge and the formation of a pile-up region was shown by RBS data to be independent of temperature in the range between $800^\circ C$ and $1000^\circ C$. Simulations using common models for the oxidation of Si and diffusion of Si in SiGe indicate that temperature does have an influence on the composition of the pile-up layer, though the range of achievable compositions is limited. The flux of Si due to diffusion of Si in SiGe relative to the oxidation-induced flux of Si out of the SiGe is integral to the formation and dimensions of a pile-up region.

Two predictive relations were derived for describing the dynamics of oxidation of SiGe. The first relation is given for determining the pile-up layer thickness as a function of oxide thickness and the composition of the pile-up layer. The second relation assumes a limited supply of Si and is for determination of the minimum initial thickness of a SiGe layer to avoid oxidation of Ge. The validity of these equations was confirmed by RBS and XPS data from this study as well as

values from TEM and XRD from other studies. The proposed models may be used in nanostructuring thin films of SiGe by oxidation and in the design of core-shell structures and transistors.

ACKNOWLEDGMENTS

The authors gratefully acknowledge the NSE-IM2NP team and NanoTecMat platform for providing the SiGe samples and the Norwegian Research Council for financial support by way of the FRINAT program.

- ¹Y. Park, G. C. King, and S. H. Choi, *J. Cryst. Growth* **310**, 2724 (2008).
- ²I. Lagnado and P. R. de la Houssaye, *Microelectron. Eng.* **59**, 455 (2001).
- ³H. S. Gamble, B. M. Armstrong, P. T. Baine, Y. H. Low, P. V. Rainey, Y. W. Low, D. W. McNeill, S. J. N Mitchell, J. H. Montgomery, and F. H. Ruddell, *Mater. Sci. Semicond. Process.* **11**, 195 (2008).
- ⁴K. L. Wang, S. G. Thomas, and M. O. Tanner, *J. Mater. Sci.: Mater. Electron.* **6**, 311 (1995).
- ⁵S. E. Thompson, M. Armstrong, C. Auth, M. Alavi, M. Buehler, R. Chau, S. Cea, T. Ghani, G. Glass, T. Hoffman, C.-H. Jan, C. Kenyon, J. Klaus, K. Kuhn, Z. Ma, B. McIntyre, K. Mistry, A. Murthy, B. Obradovic, R. Nagisetty, P. Nguyen, S. Sivakumar, R. Shaheed, L. Shifren, B. Tufts, S. Tyagi, M. Bohr, and Y. El-Mansy, *IEEE Trans. Electron Devices* **51**(11), 1790 (2004).
- ⁶S. Balakumar, K. D. Buddharaju, B. Tan, S. C. Rustagi, N. Singh, R. Kumar, G. Q. Lo, S. Tripathy, and D. L. Kwong, *J. Electron. Mater.* **38**(3), 443 (2009).
- ⁷N. Singh, K. D. Buddharaju, S. K. Manhas, A. Agarwal, S. C. Rustagi, G. Q. Lo, N. Balasubramanian, and D.-L. Kwong, *IEEE Trans. Electron Devices* **55**(11), 3107 (2008).
- ⁸A. I. Hochbaum and P. Yang, *Chem. Rev.* **110**(1), 527 (2010).
- ⁹M. Spadafora, A. Terrasi, S. Mirabella, A. Piro, M. G. Grimaldi, S. Scalse, E. Napolitani, M. Di Marino, D. De Salvador, and A. Carnera, *Mater. Sci. Semicond. Process.* **8**, 219 (2005).
- ¹⁰F. K. LeGoues, R. Rosenberg, and B. S. Meyerson, *Appl. Phys. Lett.* **54**(7), 644 (1989).
- ¹¹Y. S. Lim, J. S. Jeong, J. Y. Lee, H. S. Kim, H. K. Shon, H. K. Kim, and D. W. Moon, *Appl. Phys. Lett.* **79**(22), 3606 (2001).
- ¹²Z. Di, P. K. Chu, M. Zhang, W. Liu, Z. Song, and C. Lin, *J. Appl. Phys.* **97**, 064504 (2005).
- ¹³D. Nayak, K. Kamjoo, J. C. S. Woo, J. S. Park, and K. L. Wang, *Appl. Phys. Lett.* **56**(1), 66 (1990).
- ¹⁴J. H. Jang, S. Y. Son, W. Lim, M. S. Phen, K. Siebein, S. J. Pearton, and V. Craciun, *Appl. Phys. Lett.* **94**, 202104 (2009).
- ¹⁵B. G. Min, J. H. Yoo, H. C. Sohn, D. H. Ko, M. H. Cho, K. B. Chung, and T. W. Lee, *Thin Solid Films* **518**, 2065 (2010).
- ¹⁶Y. S. Lim, J. S. Jeong, J. Y. Lee, H. S. Kim, H. K. Shon, H. K. Kim, and D. W. Moon, *J. Electron. Mater.* **31**(5), 529 (2002).
- ¹⁷M. Spadafora, G. Privitera, A. Terrasi, S. Scalse, C. Bongiorno, A. Carnera, M. Di Marino, and E. Napolitani, *Appl. Phys. Lett.* **83**(18), 3713 (2003).
- ¹⁸J. P. Zhang, P. L. F. Hemment, S. M. Newstead, A. R. Powell, T. E. Whall, and E. H. C. Parker, *Thin Solid Films* **222**, 141 (1992).
- ¹⁹B.-G. Min, Y. H. Pae, K. S. Jun, D.-H. Ko, H. Kim, M.-H. Cho, and T.-W. Lee, *J. Appl. Phys.* **100**, 016102 (2006).
- ²⁰C. Li, K. Cai, Y. Zhang, H. Lai, and S. Chen, *J. Electrochem. Soc.* **155**(3), H156 (2008).
- ²¹T. Shimura, M. Shimizu, S. Horiuchi, H. Watanabe, K. Yasutake, and M. Umeno, *Appl. Phys. Lett.* **89**, 111923 (2006).
- ²²Y. Zhang, C. Li, K. Cai, Y. Chen, S. Chen, H. Lai, and J. Kang, *J. Appl. Phys.* **106**, 063508 (2009).
- ²³S. J. Kilpatrick, R. J. Jaccodine, and P. E. Thompson, *J. Appl. Phys.* **81**(12), 8018 (1997).
- ²⁴M. A. Rabie, Y. M. Haddara, and J. Carette, *Nanotechnology* **3**, 21 (2005).
- ²⁵M. A. Rabie, Y. M. Haddara, and J. Carette, *J. Appl. Phys.* **98**, 074904 (2005).
- ²⁶O. W. Holland, C. W. White, and D. Fathy, *Appl. Phys. Lett.* **51**(17), 520 (1987).
- ²⁷S. Tanuma, C. J. Powell, and D. R. Penn, *Surf. Interface Anal.* **20**, 77 (1993).

- ²⁸C. J. Powell and A. Jablonski, *NIST Electron Inelastic Mean Free Path Database, Version 1.1* (National Institute of Standards and Technology, Gaithersburg, MD, 2000).
- ²⁹I.-M. Lee and C. G. Takoudis, *J. Vac. Sci. Technol. A* **15**(6), 3154 (1997).
- ³⁰S. J. Kilpatrick, R. J. Jaccodine, and P. E. Thompson, *J. Appl. Phys.* **93**(8), 4896 (2003).
- ³¹R. J. Jaccodine and S. J. Kilpatrick, *Proc. Electrochem. Soc.* **2005-05**, 542 (2005).
- ³²D. C. Paine, C. Caragianis, and A. F. Schwartzman, *J. Appl. Phys.* **70**(9), 5076 (1991).
- ³³I. Barin, *Thermochemical Data of Pure Substances*, 2nd ed. (VCH, Weinheim, 1993).
- ³⁴J. E. Castle, H. D. Liu, and N. Saunders, *Surf. Interface Anal.* **20**(2), 149 (1993).
- ³⁵H. Stöhr and W. Klemm, *Z. Anorg. Allg. Chem.* **241**(4), 305 (1939).
- ³⁶J. P. Dismukes, L. Ekstrom, and R. J. Paff, *J. Phys. Chem.* **68**(10), 3021 (1964).
- ³⁷N. Daval, E. Guiot, K. K. Bourdelle, M. Kennard, I. Cayrefourcq, T. Akatsu, C. Mazure, H. Cerva, and A. Rucki, *ECS DECON* **2005-10**, 42 (2005).
- ³⁸R. Kube, H. Bracht, J. Lundsgaard Hansen, A. Nylandsted Larsen, E. E. Haller, S. Paul, and W. Lerch, *J. Appl. Phys.* **107**, 073520 (2010).
- ³⁹H. Z. Massoud, J. D. Plummer, and E. A. Irene, *J. Electrochem. Soc.* **132**(11), 2685 (1985).
- ⁴⁰B. E. Deal and A. S. Grove, *J. Appl. Phys.* **36**(12), 3770 (1965).